scientific reports

Check for updates

OPEN

Sciellin inhibits senescence and promotes pancreatic cancer progress by activating the notch signaling pathway

Changhao Wu[1,2,3,4,5,8], Dan Luo[1,2,4,5,6,8], Binbin Shi[2,4,5], Shiyu Chen[7], Chengyi Sun[1,2,3,4,5], Zhiwei He[1,3,4,5]✉ & Chao Yu[1,2,3,4,5]✉

Pancreatic cancer (PC) incidence is increasing annually globally, and the five-year survival rate of patients with PC is approximately 10%. Cellular senescence is a regulatory mechanism against cancer that prevents tumor development by inhibiting the proliferation of damaged or abnormal cells. However, the mechanisms underlying cellular senescence in PC is unclear. Sciellin (SCEL) is a precursor protein of the cornified envelope predominantly enriched in epithelial cells. Previous studies have discovered potential links between SCEL and cellular senescence through bioinformatics analysis. Therefore, the specific role of SCEL in cellular senescence and the malignant features of PC are unclear. In vivo and in vitro assays were performed to investigate the role of SCEL in PC cell senescence, proliferation, invasion, and metastasis. Gene set enrichment analysis was used to identify the Notch signaling pathways activated by SCEL, and coimmunoprecipitation was used to detect proteins that interact with SCEL. The results revealed that SCEL was significantly upregulated in PC tissues and cell models and was correlated with poor clinical outcomes. Further investigation revealed that the interaction between SCEL and Jagged-1 promotes the activation of the Notch signaling pathway, effectively inhibiting the senescence of PC cells while enhancing their proliferation, invasion, and metastatic capabilities. Therefore, SCEL is a potential therapeutic target for PC.

Keywords Pancreatic cancer, Senescence, SCEL, Jagged-1, Notch signaling pathway

Approximately 90% of pancreatic cancers (PCs) are ductal adenocarcinomas originating from the glandular duct epithelium, with insidious and atypical[1] clinical symptoms. The PC incidence has gradually increased over the past 20 years[2], and its primary therapeutic options include surgical resection, chemotherapy, and radiotherapy. However, the effectiveness of treatment is limited because early detection of PCs is complex, and the five-year survival rate is approximately 10%. Thus, PCs are one of the cancers with high mortality rates[3]. Cellular senescence has recently been identified as the primary cancer characteristic[4]. During cancer progression, cellular senescence can suppress tumor development by preventing the proliferation of damaged cells or exacerbating the tumor microenvironment through the secretion of inflammatory factors by senescent cells, thereby influencing tumor progression and treatment response[5,6]. Previous studies have demonstrated a close association between cellular senescence and the malignant behavior of PC, particularly pancreatic ductal adenocarcinoma (PDAC)[7,8]. Cellular senescence, as a complex biological process, plays a dual role in cancer development and progression: it can act as a tumor suppressor by inhibiting the proliferation of damaged cells and senescent cells can promote the formation and development of the tumor microenvironment through their senescence-associated secretory phenotype, releasing various pro-inflammatory factors and other bioactive molecules, thereby influencing tumor progression and treatment response[9]. Therefore, cellular senescence may be a key mechanism underlying

[1]Department of Hepatobiliary Surgery, The Affiliated Hospital of Guizhou Medical University, Guizhou Medical University, Guiyang 550001, China. [2]College of Clinical Medicine, Guizhou Medical University, Guiyang 550001, China. [3]Guizhou Provincial Institute of Hepatobiliary, Pancreatic and Splenic Diseases, Guiyang 550001, China. [4]Key Laboratory of Liver, Gallbladder, Pancreas and Spleen of Guizhou Medical University, Guiyang 550001, China. [5]Guizhou Provincial Clinical Medical Research Center of Hepatobiliary Surgery, Guiyang 550004, Guizhou, China. [6]Department of Hepatobiliary Surgery, People's Hospital of the Guizhou Province, Guiyang 550003, China. [7]Department of Hepatic-Biliary-Pancreatic Surgery, Medical School, South China Hospital, Shenzhen University, Shenzhen 518116, China. [8]Changhao Wu and Dan Luo contributed equally to this work. ✉email: 2268272794@qq.com; yuchao2002@gmc.edu.cn

PC cell proliferation, drug resistance, and metastasis; however, the molecular mechanisms regulating senescence in tumor cells are not understood.

The Notch gene was named based on genetic studies in *Drosophila melanogaster* (fruit fly), in which loss-of-function mutations in this gene resulted in Notched wing margins. A previous study confirmed the close relationship between Notch mutations and cancer[10]. Notch signaling regulates hematopoiesis and immune cell differentiation and is associated with various autoimmune diseases, tumorigenesis, and tumor-induced immune suppression. Although the Notch signaling pathway is simple, its cellular processes are complex. Mutations in Notch genes have been identified in multiple types of tumors through genome sequencing. Aberrantly activated Notch signaling is involved in virtually all the fundamental characteristics of cancer, including tumor angiogenesis, cancer stemness, and epithelial-mesenchymal transition[11]. The canonical Notch signaling pathway transmits signals through cell-to-cell contact and is known as the recombination signal-binding protein J (RBP-J)-dependent pathway, which requires Notch receptors, ligands, RBPJ, and target genes[12]. In mammals, binding of Notch receptors (Notch1, Notch2, Notch3, and Notch4) to their ligands (Jagged1, Jagged2, DLL1, DLL3, and DLL4) initiates Notch signaling. Jagged-1 is a key ligand of the Notch pathway and is highly expressed in PC[13]. It promotes cancer cell proliferation and metastatic potential and regulates immunosuppressive tumor-associated macrophage function. The Notch signaling pathway, especially through Notch-1 and its ligand Jagged-1, regulates epithelial cell senescence[14]. Inhibition of Notch signaling induces premature senescence through a p16-dependent pathway, whereas overexpression of Notch-1 or Jagged-1 prolongs the replicative lifespan of these cells[15]. The mechanisms by which the Notch pathway participates in tumor senescence, promoting PC progression, are not understood.

Sciellin (SCEL), a cornified envelope precursor, is predominantly enriched in the epithelial cells and plays a significant role in the pathogenesis of cancer and other diseases[16]. Previous studies have indicated that SCEL is involved in cell proliferation and neutrophil extracellular trap formation in gallbladder cancer[17]. Guo et al. demonstrated that SCEL promoted the progression of thyroid cancer through the Janus kinase 2/signal transducer and activator of the transcription 3 signaling pathway[18]. Chan et al. indicated that SCEL regulates triple-negative breast cancer lung metastasis via the tumor necrosis factor-α/tumor necrosis factor receptor 1/nuclear factor-κB/FLICE-like inhibitory protein axis[19]. Additionally, SCEL mediates angiogenesis and promotes wound healing in burn injuries through the homebox transcript antisense RNA/miR-126 axis[20]. Cheng et al. highlighted the potential of SCEL as a diagnostic marker and therapeutic target for PC, although its specific mechanism of action is unclear[21]. Therefore, we hypothesized that SCEL inhibits cellular senescence and promotes PC cell proliferation, invasion, and metastasis by activating the Notch signaling pathway through its interaction with Jagged-1.

Materials and methods

Bioinformatics analysis

The Cancer Genome Atlas and genotype-tissue expression databases were integrated into the Gene Expression Profiling Interactive Analysis (GEPIA) platform. Gene set enrichment analysis was used for comprehensive gene association studies.

Collection of pancreatic cancer samples

One hundred and four paired PC and adjacent non-tumorous pancreatic tissue samples were collected with the approval of the Guizhou Medical University ethics committee (approval number: 2023-069). Informed consent was obtained from all the subjects. All procedures and methods were performed in accordance with relevant guidelines and regulations, including the Helsinki Declaration.

Immunohistochemistry protocol

The tissue samples were subjected to various preparatory steps, including fixation, embedding, deparaffinization, and blocking. The samples were incubated with primary antibodies, such as anti-SCEL and -KI67, overnight at 4 ℃, and the details are specified in the Supplementary Table. Following incubation with the primary antibody, the tissues were exposed to secondary antibodies and counterstained with Mayer's Hematoxylin Stain solution (G1080, Solarbio, Beijing, China). The immunoreactive score was used to quantify immunohistochemistry (IHC) staining, it ranges from 0 to 12, and is calculated by multiplying the positive cell proportion (0:0%, 1: <20%, 2:20–40%, 3: 40–60%, 4: > 60%) and staining intensity scores (0: negative, 1: weak, 2: moderate, 3: strong).

RNA extraction and real-time quantitative polymerase chain

RNA was isolated using Trizol (Life Technologies, Carlsbad, CA, USA), followed by quantification and cDNA synthesis using the NanoDrop ND1000 (Thermo Fisher Scientific, Waltham, MA, USA) and TransScript Two-Step real-time quantitative polymerase chain (qPCR) SuperMix (Thermo Fisher Scientific). qPCR was performed using PerfectStart Green qPCR SuperMix (Thermo Fisher Scientific), with expression levels determined using the $2-\Delta\Delta CT$ method. The primer sequences used in the study were: SCEL GAPDH (internal control) primer (forward primer, 5′-CTCCAAAATCAAGTGGGGCG-3′; reverse primer, 5′-TGGTTCACACCCATGACGAA-3′); SCEL primer (forward primer, 5′-GTGCTCAACCGACATAATTCCC-3′; reverse primer, 5′-TGTCATCAG AACTGTACCGACTA-3′); Jagged-1 primer (forward primer, 5′-GTCCATGCAGAACGTGAACG-3′; reverse primer, 5′-GCGGGACTGATACTCCTTGA-3′). Jagged-1 primer (forward primer, 5′-GTCCATGCAGAACGT GAACG-3′; reverse primer, 5′-GCGGGACTGATACTCCTTGA-3′).

Protein analysis using Western blotting

Proteins were extracted from cell lysates using radioimmunoprecipitation assay buffer (R0010; Solarbio), and protein concentrations were determined using a bicinchoninic acid assay. Sodium dodecyl-sulfate-polyacrylamide

gel electrophoresis facilitated protein separation and transfer onto polyvinylidene fluoride membranes. Next, block with 5% non-fat milk solution for 1 h, incubated with the corresponding primary antibody overnight at 4 ℃, then incubated with the secondary antibody (Proteintech, Rosemont, IL, USA) at room temperature for 2 h, and observed using a MeilunbioWest Femto Maximum Sensitivity Substrate (MA0187, Meilunbio, Liaoling, China) and band intensity was measured using ImageJ (National Institute of Health, Bethesda, ML, USA). All the gels were analysis and statistics based on grayscale value, and the results were shown in Supplementary Material 1. S4-5. The original images of gels and the details of the antibodies and dilutions used are listed in Supplementary Material 2–3.

Cell culture

Five PC cell lines (Excellos, Manassas, VA, USA) and one human pancreatic nestin-expressing cell line were cultured under specific conditions and supplemented with 10% fetal bovine serum (FBS [Gibco, Waltham, MA, USA]). Authentication was done using short tandem repeat profiling.

Cell transfection

Gene expression was modulated using short hairpin RNA, small interfering RNAs, and overexpression plasmids, and transfection was performed using Lipofectamine 3000 (Invitrogen Life Technologies, Waltham, MA, USA). Specifically, according to the manufacturer's instructions, short hairpin RNA and Lipofectamine 3000 (Invitrogen) were diluted separately in Opti-MEM (31985070 [Thermo Fisher Scientific]), thoroughly mixed, incubated at room temperature for 15 min, and then uniformly added to the culture system, incubated for a period, until subsequent experiments. The transfection methods used for small interfering RNA and overexpression plasmids were similar to those described above. The short hairpin and small interfering RNA sequences of SCEL were sh1:5′-CATTGATCTGGAGAACATTGT-3,' sh2:5′-GTACCTGATGACCATGATAGC-3′,' The small interfering RNA of SCEL as si1:5′- CCAAGTTACTTTGCTTGTCTGA-3′.'

Cell proliferation assay

Three thousand PC cells were seeded per well in a 96-well plate and cultured for 0, 24, 48, or 72 h. Next, the Cell Counting Kit-8 reagent (CCK-8 [Dojindo Molecular Technologies, Inc., Tokyo, Japan]) was added to the medium at a ratio of 1: 10 (10 μL per well). After incubation for 2 h, absorbance was measured at 450 nm using a microplate reader (Tecan, Viena, Austria). Five wells represented each group, and the analysis was independently conducted thrice.

Assessment of cellular senescence

The senescence β-galactosidase staining kit (C0602, Beyotime Biotechnology, Shanghai, China) was used to detect senescent cells in lysates and tissue extracts. After fixing the cells, the staining working solution was added, following incubation with assay buffer at 37 ℃ for 24 h. The cells were observed under and imaged using an optical microscope (Nikon, Tokyo, Japan). Next, the total number of cells and the number of β-galactosidase-stained positive cells within the field of vision were recorded. The percentage of positive cells was calculated using the following formula: percentage of positive cells = n/N where N is the total number of cells and n is the number of β-galactosidase-stained positive cells.

Evaluation of DNA synthesis

5-Ethynyl-2′-deoxyuridine (EdU) incorporation assays were conducted to measure active DNA synthesis. Briefly, PC cells were plated onto a 24-well culture plate and cultured until they reached a certain degree of confluency. Next, 10 μM EdU solution (Sigma-Aldrich, St Louis, MI, USA) was added, and the mixture was incubated for 2 h. Cells were fixed and washed with 4% paraformaldehyde for 15 min and phosphate-buffered saline (PBS [Invitrogen]), respectively. The cells were permeabilized with 0.5% Triton X-100 Solution (ST797, Beyotime) for 10 min, washed with PBS (Invitrogen), incubated with the click reaction solution (Beyotime) for 30 min, and rewashed with PBS (Invitrogen). Nuclear staining was performed using 4′,6-diamidino-2-phenylindole (DAPI [C0065, Solarbio]), and the results were observed and recorded under and using a fluorescence microscope (Nikon), respectively. The percentage of positively stained cells is the percentage of EdU- relative to DAPI-positive cells.

Colony formation assay

For colony formation assessment, the cells were plated in 6-well plates, allowing colony development before staining and evaluation, and the captured images were analyzed using the ImageJ software (National Institute of Health) to quantify the number of colonies.

Immunofluorescence analysis

The cells were fixed and permeabilized before staining with immunofluorescence markers, incubated with bovine serum albumin (Invitrogen) at room temperature for 1 h, and washed thrice with Phosphate-Buffered Saline with Tween 20 (PBST [Sigma-Aldrich]). Next, the cells were incubated with the primary antibody overnight at 4 ℃, followed by incubation with the secondary antibody at room temperature for 1 h. After washing thrice with PBST, nuclear staining was performed using DAPI. A confocal microscope (Carl Zeiss, Jena, Germany) was used for imaging. Fluorescence intensity was quantified using ImageJ (National Institute of Health), and Origin software (OriginLab Corporation, Northampton, MA, USA) was used to plot curves.

Assessment of cell migration

The wound-healing assay was applied to confluent cell monolayers to evaluate cell migration capabilities, and observations were made over 48 h. The images were processed using ImageJ (National Institute of Health) to acquire migration data, and the relative migration ability was calculated using the following formula: relative migration ability = (wound area at 48 h) / (wound area at 0 h) × 100%. GraphPad Prism 9 (GraphPad, San Diego, CA, USA) was subsequently used for statistical analysis and to generate graphs.

Transwell migration and invasion assays

Transwell chambers were placed on a 24-well plate for Transwell assays. Firstly, 2×10^4 PC cells were seeded in the upper chamber and cultured in 200 μL of serum-free medium. For invasion experiments, the upper membrane was covered with a Matrigel before cell seeding. Subsequently, 600 μl Dulbecco's Modified Eagle Medium (Thermo Fisher Scientific) + 10% FBS (Gibco) to the lower chamber. After incubation at 37 ℃ for 24 h, the Transwell chambers were washed with PBS, fixed with 4% paraformaldehyde for 30 min, rewashed with PBS, and stained with crystal violet (Sigma-Aldrich) for 30 min. Images of each Transwell chamber were captured using a microscope (Nikon), and the number of stained cells in the images was measured using ImageJ software (National Institute of Health). Statistical charts were generated using GraphPad Prism 9 (GraphPad).

In vivo experimental models

Six-week-old female BALB/c nude mice (HFK Bio-Technology Co., Ltd, Beijing, China) were used for tumor xenograft and metastasis experiments in compliance with ethical standards. Monitoring of tumor growth and metastatic spread was systematic, as depicted in the schematics provided. The animals were euthanized using isoflurane, and all efforts were made to minimize their suffering. All animal experiments were approved by the Laboratory Animal Ethics Committee of the Guizhou Medical University (approval number: 2304337). All methods used in animal experiments were carried out considering relevant guidelines, handled according to standard protocols and animal welfare regulations, and reported considering ARRIVE guidelines (http://arriveguidelines.org) for reporting animal experiments. SCEL control or ASPC-1 cells with SCEL knockdown (2×10^6 cells) were injected subcutaneously into nude mice. Tumors were measured weekly for 5 weeks using an External Caliper, and tumor volume was calculated using the following formula: $(L \times W^2)/2$. At the end of the experiment, the tumors were excised for subsequent experiments. To establish lung metastasis assays, ASPC-1 cells with SCEL control or knockdown (1×10^6 cells) were injected via the lateral tail vein into nude mice (seven mice per group), and the experiment was conducted for 6 weeks. At the end of the experiment, the lung tissues were removed and stained with hematoxylin and eosin (Sigma-Aldrich) for histological confirmation of metastatic tumor cells.

Coimmunoprecipitation technique

Transfected cells expressing different expression vectors were lysed in NP-40 lysis buffer (N8032, Solarbio) containing protease inhibitors at 4 ℃ for 30 min, followed by centrifugation at 12,000 *g* for 15 min at 4 ℃. The supernatant was incubated with anti-FLAG Magnetic beads (HAK21011, HUABIO, Woburn, MA, USA) overnight at 4 ℃. After collection, the magnetic beads were washed thrice with Tris-buffered saline (Sigma-Aldrich) at a ration of 10 :1 by volume. Next, 10 μL of the original magnetic bead volume was mixed with 50 μL of 1X Sodium dodecyl sulfate-polyacrylamide gel electrophoresis (SDS-PAGE) loading buffer (Thermo Fisher Scientific), heated at 95 ℃ for 10 min. The beads were then placed on a magnetic stand for separation until the solution was clear, and the supernatant was collected for SDS-PAGE and Western Blot analysis.

Notch pathway inhibitor disitrubin Analog peptide T

Disitrubin Analog Peptide T (DAPT) solution (HY-13027, MedChemExpresss, Monmouth Junction, NJ, USA) inhibits the γ-secretase activity of Notch receptors, subsequently inhibiting the Notch signaling pathway. DAPT was dissolved in Dimethyl sulfoxide, and the cells were plated and grown steadily. Then, they were treated with 10 mM DAPT solution (MedChemExpress) in the culture system. Subsequent experiments were conducted 48 h after treatment.

Tumor volume calculation

The tumor volume was calculated using the following formula: Volume (mm^3) = (length (mm) × (width (mm))^2) / 2. This formula is based on the measurement of two perpendicular diameters of the tumor, where the length is the longest diameter and the width is the shortest diameter perpendicular to the length. This method provides a reliable estimate of the tumor volume, which is crucial for monitoring tumor growth over time.

Subcutaneous tumor model establishment

Six-week-old BALB/c nude mice were used to establish a subcutaneous Pancreatic ductal adenocarcinoma (PDAC) tumor model. The mice were injected subcutaneously with 1 × 10^6 ASPC cells, a PC cell line, and iN 100 μL of sterile PBS (Invitrogen) into the right flank region. Tumor growth and progression were monitored regularly, and the mice were weighed and observed daily for signs of distress or illness.

Pulmonary metastasis model establishment

To develop a pulmonary metastasis model of PDAC, 6-week-old BALB/c nude mice were injected with 1 × 10^6 ASPC3 cells via the tail vein to induce lung metastasis. The cells were suspended in 100 μL of sterile PBS (Invitrogen) to simulate the natural route of metastasis and allow the study of tumor cell behavior in a live model.

Statistical analysis

Data were analyzed and presented using conventional statistical methods, including Student's t-test for comparative analyses and Kaplan–Meier plots for survival studies, with Pearson's correlation analysis to evaluate the association between SCEL and Jagged-1. All data are presented as means ± standard deviation (SD) of three independent experimental replicates. All statistical analyses were performed using GraphPad Prism 9 (GraphPad). Statistical significance was defined at ns-$P > 0.05$, *$P < 0.05$, **$P < 0.01$. ***$P < 0.001$, ****$P < 0.0001$.

Results

Enhanced sciellin expression in early pancreatic cancer

Using data from the GEPIA database, which comprises 179 PC and 171 normal pancreatic specimens, we observed a notable increase in SCEL expression in PC tissues (Fig. 1A). This elevated expression was inversely correlated with overall and disease-free survival, with patients exhibiting higher SCEL levels and shorter survival durations than those of the control (Fig. 1B, C). Ascending and decreasing trends in SCEL expressions were noted in stages I–III and IV, respectively, (Supplementary Material 1. S1A). Furthermore, an analysis integrating multiple databases underscored the diagnostic and prognostic value of SCELs, demonstrating enhanced predictive accuracy for 1-, 3-, and 5-year survival rates (Fig. 1D, E). Corroborating these findings, examination of 104 samples from patients with PC revealed that elevated SCEL expression was associated with poor survival outcomes (Fig. 1F). Analysis of clinical data and IHC results revealed a significant association between increased SCEL levels and more advanced tumor (T) and nodal (N) stages. However, there was no significant correlation with the metastatic (M) stage (Fig. 1G–I). Intriguingly, although SCEL expression increased in stages I–III, its upregulation was not pronounced at stage IV (Fig. 1J). Additional validation through western blotting and IHC of PC and adjacent non-tumorous tissues confirmed the significant upregulation of SCEL in PC tissues (Fig. 1K, L). Comparative analyses at the mRNA and protein levels revealed that SCEL expression was substantially higher in PC cells than that in human pancreatic nestin-expressing cells (Supplementary Material 1. S1B and S1C). Collectively, these findings underscore the pronounced expression of SCEL during the PC nascent stages, suggesting their role as pivotal biomarkers for early disease detection and progression.

Sciellin inhibits senescence in pancreatic cancer cells

Stable SCEL-knockdown models were established in AsPC-1 and Mia PaCa-2 PC cell lines to elucidate the role of SCELs in PC cellular senescence. The efficacy of SCEL suppression was validated using qPCR and western blot analyses, focusing on the sh-SCEL#1 and sh-SCEL#2 constructs (Fig. 2A, B). Subsequent analyses revealed that the abrogation of SCEL expression precipitated an induction of cellular senescence, as revealed by immunofluorescence (Fig. 2C, D) and β-galactosidase staining (Fig. 2E) results. Additionally, western blotting further elucidated the senescence mechanism, exhibiting upregulation of the senescence marker protein P21 and a concomitant decrease in lamin B1, a protein associated with nuclear structure and cellular integrity (Fig. 2F). Collectively, these findings demonstrate the SCEL anti-senescence function in PC cells in vitro, indicating its pivotal role in modulating cellular aging processes in PC.

Sciellin facilitates pancreatic cancer cell growth and metastatic potential

Investigations into the role of SCEL in PC cell dynamics revealed that it promotes cell proliferation and metastasis. Cell growth was assessed using in vitro assays, including the CCK-8, colony formation, and EdU incorporation assays, demonstrating that SCEL knockdown significantly attenuated cell proliferation (Fig. 3A–C). Furthermore, assessments of cell migratory and invasive potential via wound healing and Transwell migration assays confirmed that SCEL silencing markedly impaired the migratory and invasive capacities of PC cells (Fig. 3D, E). Collectively, these findings elucidate the pivotal role of SCEL in augmenting the invasive and metastatic behavior of PC cells and underscore its influence on the aggressive phenotypic characteristics of PC in vitro.

Sciellin modulates pancreatic cancer senescence, proliferation, and metastasis in vivo

In vivo analyses using subcutaneous tumor models and lung metastasis assays in nude mice were conducted to explore the effects of SCEL on PC senescence, proliferation, and metastatic behavior (Fig. 4A). Mice inoculated with AsPC-1 cells exhibiting silenced SCEL expression developed significantly smaller subcutaneous tumors after a 5-week observation period, as evidenced by reduced tumor size and weight compared with those of the controls (Fig. 4B–D). IHC evaluations further substantiated these findings, exhibiting a decrease in proliferation markers (Ki-67 and proliferating cell nuclear antigen) and a metastatic marker (N-cadherin), along with an increase in the senescence-associated marker, lamin B1, in tumors derived from the SCEL-suppressed group (Fig. 4E, F). Additionally, a lung metastasis model in nude mice revealed that SCEL silencing markedly reduced the incidence of lung metastasis, confirming its role in promoting metastasis in vivo (Fig. 4G, H). These in vivo studies underscore the dual role of SCEL in repressing senescence and facilitating PC cell proliferation and metastasis, highlighting their potential as therapeutic targets for PC management.

Sciellin enhances pancreatic cancer growth via notch pathway activation and Jagged-1 stabilization

Gene set enrichment analysis was conducted using The Cancer Genome Atlas data from patients with pancreatic ductal adenocarcinoma stratified by SCEL expression levels to investigate the mechanisms underlying the SCEL facilitation of PC growth. The analysis revealed significant alterations in the Notch signaling pathway, suggesting its crucial involvement in tumor proliferation (Fig. 5A). Subsequent integrative analyses, including correlation assessments, differential expression studies, and prognostic evaluations, identified Jagged-1 as a critical effector of the Notch pathway, which is influenced by the SCEL activity (Supplementary Material 1. S2A–E). Data from

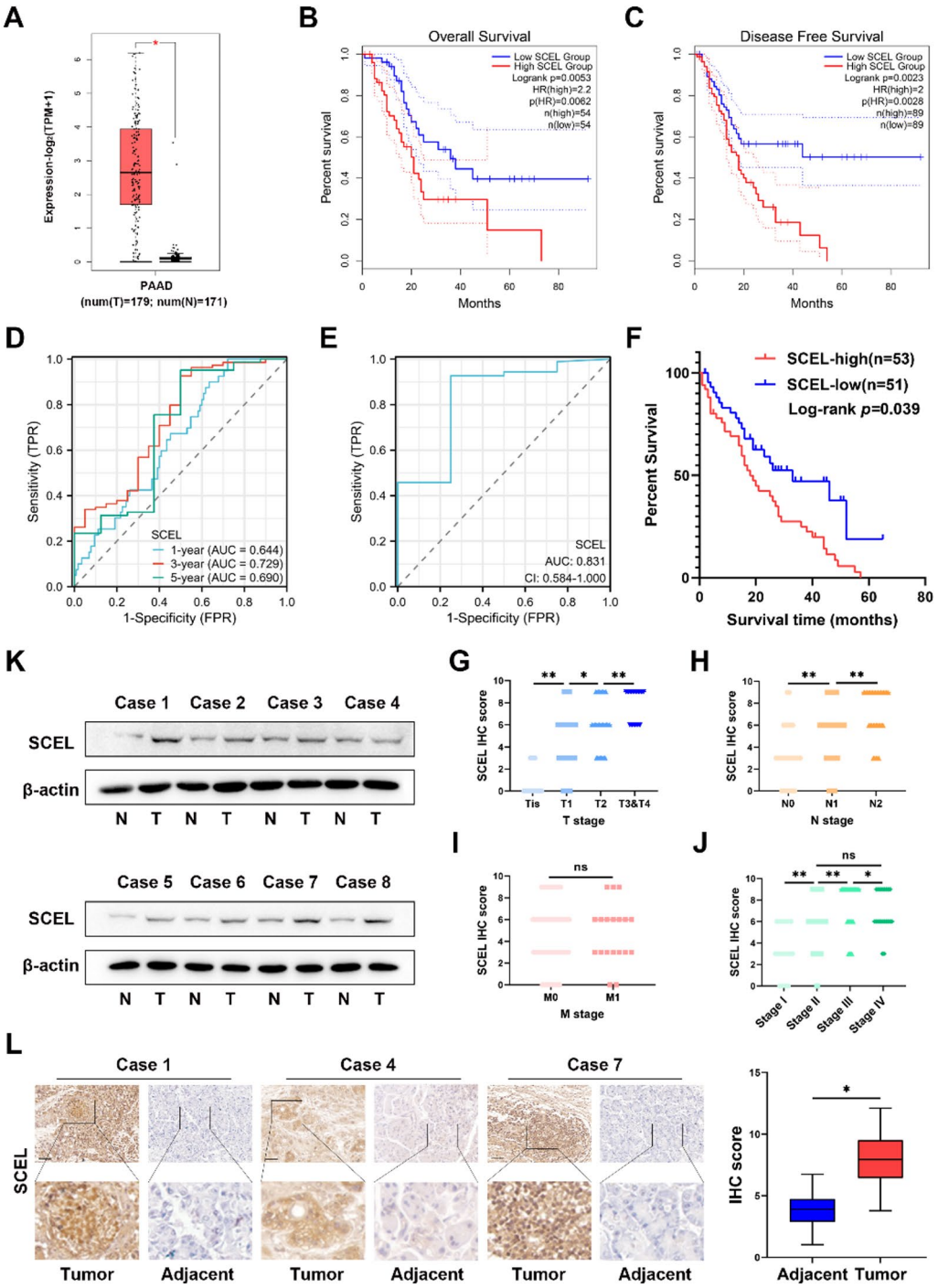

Fig. 1. Elevated Sciellin expression in pancreatic cancers highlights its early disease involvement and prognostic impact. Analysis of the pancreatic cancer (PC) public dataset, encompassing 179 PC specimens and 171 control pancreatic tissues, was conducted using the Gene Expression Profiling Interactive Analysis database, illustrating (**A**) differential expression of SCELs, (**B**) variations in overall survival duration, and **C** disparities in the disease-free survival interval. Assessment of the prognostic value of sciellin (SCEL) through time-dependent receiver operating characteristic (ROC) curves (**D**) and diagnostic potential using ROC analysis (**E**). (**F**) Kaplan–Meier survival analysis of 104 patients with pancreatic cancer categorized considering the immunohistochemistry (IHC) scoring. The correlations between SCEL expression and tumor progression parameters, including the T (**G**), N (**H**), M (**I**), and cumulative stages (**J**), were determined considering clinical data and corresponding IHC findings. SCEL comparative expression in pancreatic cancer and adjacent non-neoplastic tissues was evaluated using western blot analysis (**K**) and IHC assessment (**L**). The data on the three biologically independent samples were analyzed using analysis of variance. *, **, ***, and **** represent $P < 0.05$, $P < 0.01$, $P < 0.001$, and $P < 0.0001$ significance levels.

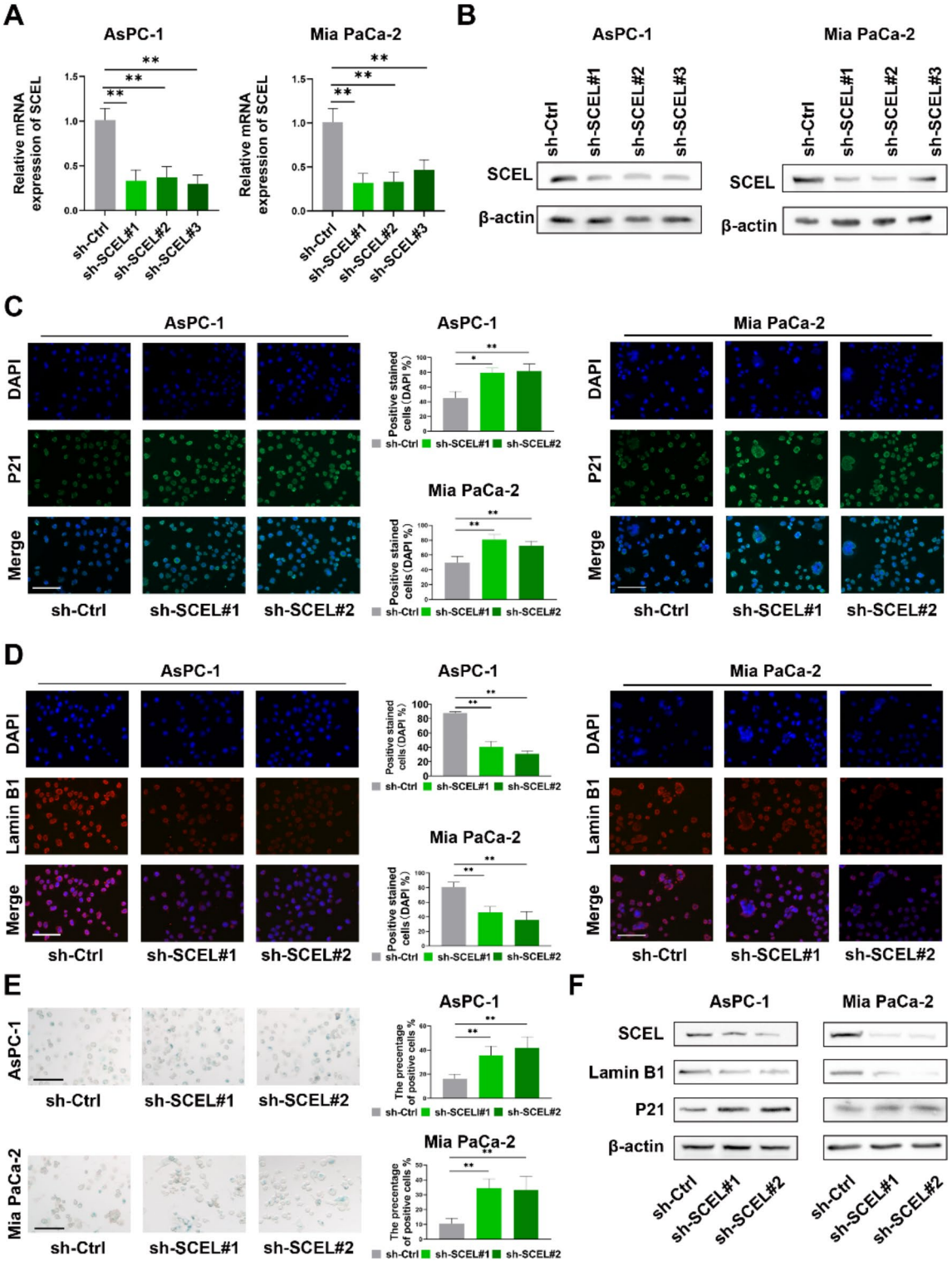

Fig. 2. Sciellin mitigation of pancreatic cancer cellular senescence in vitro. This figure presents the Sciellin (SCEL) role in reducing senescence in AsPC-1 and Mia PaCa-2 pancreatic cancer cells. (**A**) Real-time quantitative polymerase chain reaction analysis indicates the mRNA expression levels of SCEL, while (**B**) western blotting further elucidates SCEL protein expression. Immunofluorescence assays (**C**,**D**) were performed to quantify the senescence-associated protein concentrations in both cell types. (**E**) β-galactosidase staining delineates senescence in the specified cells. (**F**) Western blot analysis provides a comparative overview of lamin B1, P21, and SCEL protein expression levels. The data on the three biologically independent samples were analyzed using analysis of variance. *, **, ***, and **** represent $P<0.05$, $P<0.01$, $P<0.001$, and $P<0.0001$ significance levels.

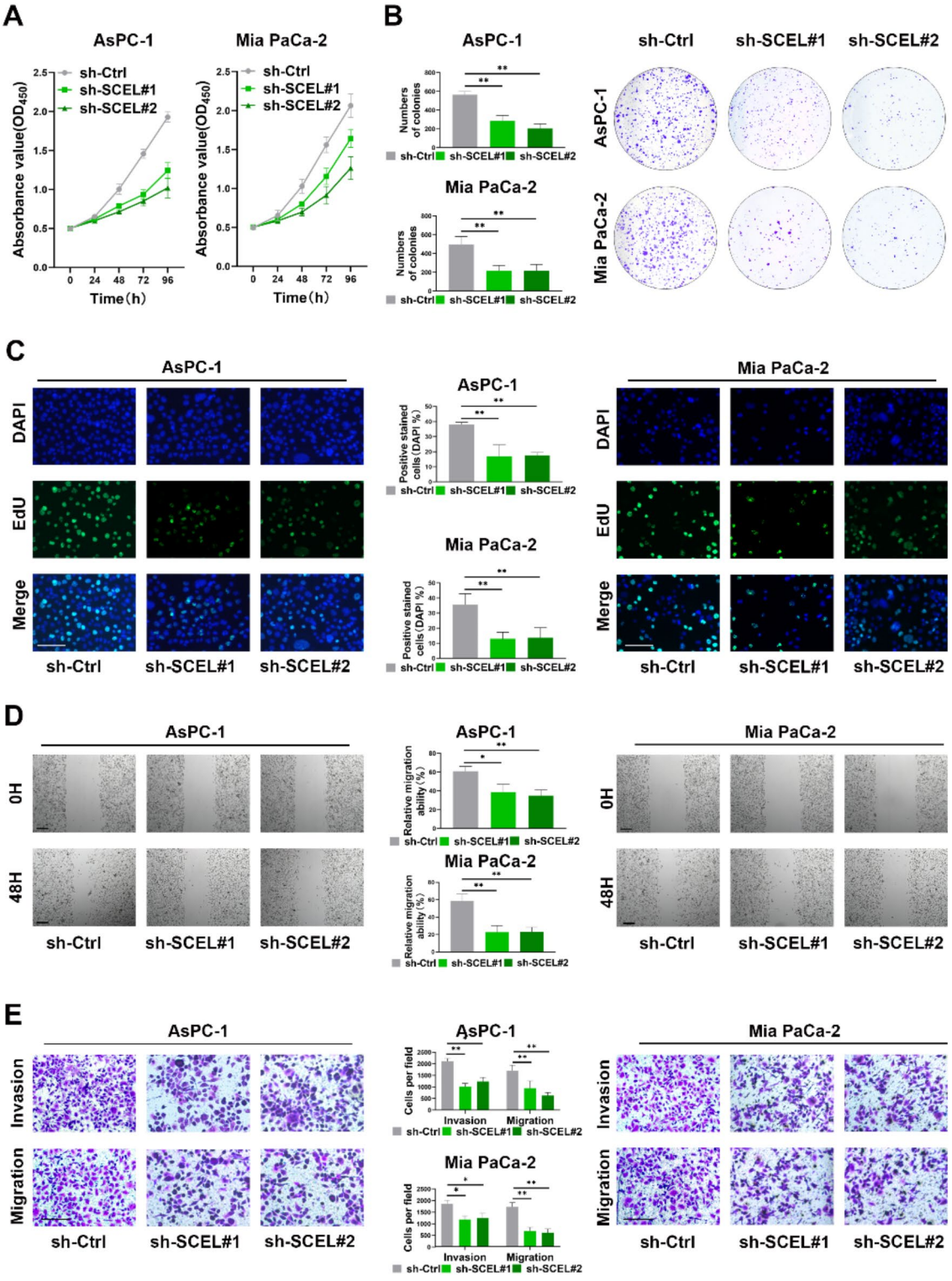

Fig. 3. Sciellin facilitation of pancreatic cancer cell proliferation and metastasis *in vitro.* Figure 3 illustrates the sciellin (SCEL) contribution to pancreatic cancer (PC) cell proliferation and metastasis. (**A**) Cell Counting Kit-8 assay was used to determine cell viability in the specified cell groups. (**B**) Photographic representation of the colonies formed by PC cells, underscoring their proliferation. (**C**) 5-Ethynyl-2′-deoxyuridine staining images exhibiting active DNA synthesis as a marker for cell proliferation. (**D**) Wound healing assay results for AsPC-1 and Mia PaCa-2 cell lines illustrating migration capabilities indicative of metastatic potential. (**E**) Transwell migration assays provide visual evidence of enhanced cell migration and invasion in response to SCEL expression. The data on the three biologically independent samples were analyzed using analysis of variance. *, **, ***, and **** represent $P < 0.05$, $P < 0.01$, $P < 0.001$, and $P < 0.0001$ significance levels.

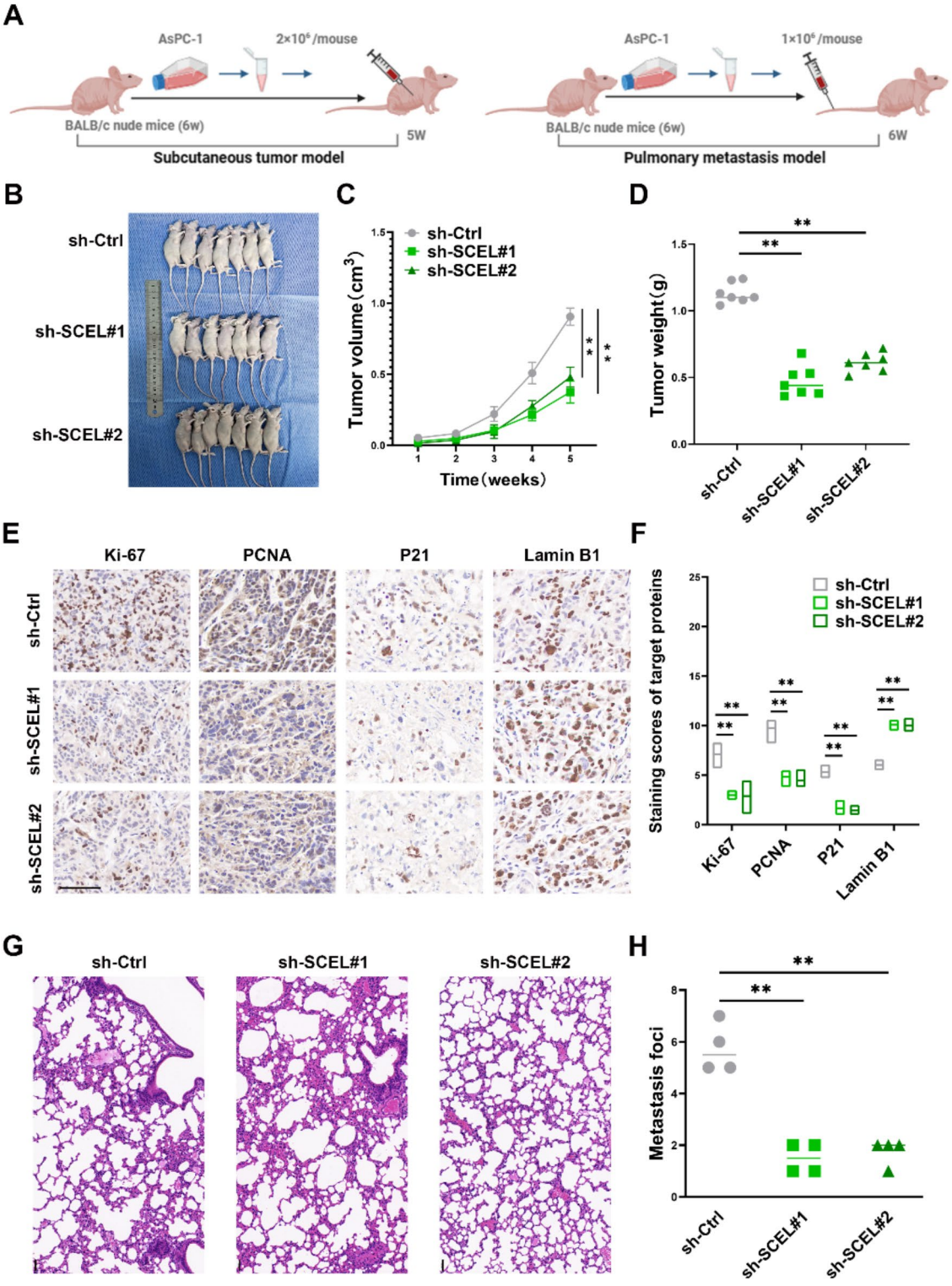

Fig. 4. Dual role of sciellin in attenuating senescence and enhancing proliferation and metastasis of pancreatic cancer cells in vivo. (**A**) Overview of the study design presenting a model of tumor growth and metastasis. (**B**) Images illustrating tumors formed in mice injected with specific pancreatic cancer cells. (**C**) Growth curves of tumors over time. (**D**) Final tumor weights. (**E**) Immunohistochemistry (IHC) identifies key protein expression—Ki-67, proliferating cell nuclear antigen (), P21, and lamin B1 (senescence markers)in tumors. (**F**) Scores from IHC quantifying protein levels; scale bar: 50 m. (**G**) Images highlighting lung metastases, with a larger scale for clarity; scale bar: 500 m. (**H**) Microscopic evaluation of hematoxylin and eosin-stained lung sections revealed metastatic foci (indicated by arrows), with counts reflecting the number of sites. The data on the three biologically independent samples were analyzed using analysis of variance. *, **, ***, and **** represent $P < 0.05$, $P < 0.01$, $P < 0.001$, and $P < 0.0001$ significance levels.

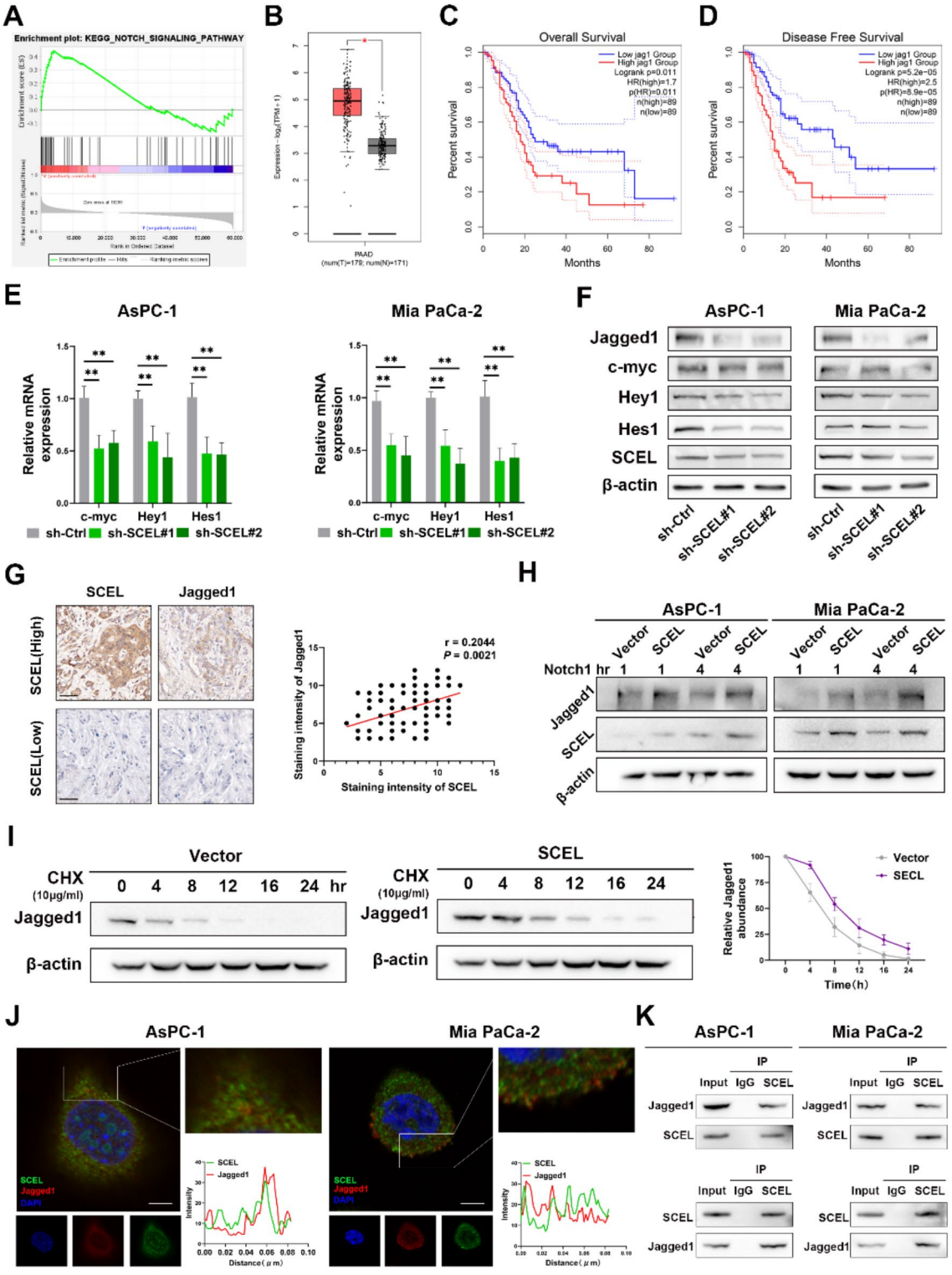

public repositories confirmed Jagged-1 overexpression in PC specimens, correlating elevated levels with reduced overall and disease-free survival (Fig. 5B–D). qPCR and western blotting revealed that SCEL overexpression was upregulated, whereas its silencing downregulated the expression of downstream targets of the Notch signaling (Hes1, Hey1, and c-myc) pathway (Fig. 5E, F and Supplementary Material 1. S3C). Exploration into the regulation of Jagged-1 by SCEL revealed no significant changes at the mRNA level after SCEL modulation (Supplementary Material 1. S3A and S3B); however, Jagged-1 protein levels were positively correlated with SCEL expression (Fig. 5F and Supplementary Material 1. S3C). Additionally, tissue arrays from 40 PC samples revealed that Jagged-1 protein levels were positively correlated with SCEL protein levels (Fig. 5G). The post-transcriptional enhancement of Jagged-1 expression by SCEL was further investigated by administering a Notch pathway agonist (Notch1) to SCEL-overexpressing cells, which increased Jagged-1 expression over time (Fig. 5H). Additionally, the stability of the Jagged-1 protein in SCEL-overexpressing AsPC-1 cells was assessed

◀**Fig. 5**. Activation of Notch signaling by sciellin through Jagged-1 protein stabilization enhances pancreatic cancer growth. This figure illustrates the mechanism by which sciellin (SCEL) promotes pancreatic cancer (PC) growth, focusing on activating the Notch signaling pathway and stabilizing Jagged-1 protein expression. (**A**) Gene Set Enrichment Analysis highlights the Notch signaling pathway enrichment in differentially expressed genes. (**B–D**) Gene Expression Profiling Interactive Analysis database analysis revealed Jagged-1's differential expression in PC and its correlation with overall and disease-free survival times. (**E**,**F**) qPCR and western blot analyses demonstrate the expression of Notch signaling pathway targets across the various treatment groups. (**G**) immunohistochemistry assays on successive tissue sections revealed SCEL and Jagged-1 expression when 40 samples were analyzed using Pearson's chi-squared method. (**H**) Western blot revealed SCEL and Jagged-1 expression after stimulation with a Notch agonist. (**I**) Western blotting was used to track Jagged-1 stability post-cycloheximide treatment of SCEL-overexpressing AsPC-1 cells. (**J**) Immunofluorescence microscopy exhibiting SCEL and Jagged-1 colocalization in the cytoplasm, highlighting their interactions. (**K**) Coimmunoprecipitation confirmed SCEL-Jagged-1 protein interaction in AsPC-1 and Mia PaCa-2 cells. The gray level was quantified using the ImageJ software. The data are presented as the mean ± standard deviation of three independent experiments. Scale bar: 100 μm (**G**), 10 μm (**J**). The data on the three biologically independent samples were analyzed using analysis of variance. *, **, ***, and **** represent $P < 0.05$, $P < 0.01$, $P < 0.001$, and $P < 0.0001$ significance levels.

after treatment with the protein synthesis inhibitor, cycloheximide, revealing that the presence of SCEL bolstered Jagged-1 stability (Fig. 5I). Immunofluorescence staining confirmed SCEL and Jagged-1 colocalization and enhanced Jagged-1 expression in PC cells overexpressing SCEL (Fig. 5J and Supplementary Material 1. S3D). Coimmunoprecipitation assays revealed a direct interaction between SCEL and Jagged-1, suggesting that SCEL protects Jagged-1 from proteasomal degradation (Fig. 5K). These findings underscore the critical function of SCEL in promoting PC growth through activation of the Notch signaling pathway, primarily by stabilizing Jagged-1 protein expression, thereby outlining a novel regulatory mechanism of tumor progression.

Sciellin augments pancreatic cancer progression through notch signaling activation

We investigated the involvement of the Notch signaling pathway using small interfering RNA against Jagged-1 (si-Jagged1) and the Notch pathway inhibitor DAPT (10 mM) to elucidate the mechanism underlying the role of SCEL in PC progression. The outcomes from immunofluorescence and β-galactosidase assays indicated that the abrogation of Jagged-1 expression and the inhibition of Notch signaling markedly mitigated the SCEL-mediated suppression of PC cell senescence (Fig. 6A–F), consistent with immunoblotting results (Fig. 6G). Furthermore, cell viability and proliferation assessments conducted via CCK-8, colony formation, and EdU incorporation assays, and cell migration and invasion evaluations using Transwell and wound healing assays confirmed that targeting Jagged-1 and inhibiting the Notch pathway significantly counteracted the proliferative and metastatic effects induced by SCEL in PC cells (Fig. 7A–I). Collectively, these findings highlight that Jagged-1 and its pivotal function within the Notch signaling cascade are critical mediators of the influence of SCEL on the oncogenic attributes of PC cells, underscoring the potential therapeutic value of targeting this pathway in PC treatment.

Discussion

PC is a highly malignant, incurable, and aggressive disease with a high mortality rate[1]. Despite advances in treatment strategies, including surgery, chemotherapy, radiotherapy, targeted therapy, and combination treatment regimens, the 5-year survival rate of PC is extremely low[3,22]. Therefore, new treatment modalities are urgently needed. The association between cellular senescence and cancer primarily manifests in the ability of senescent cells to inhibit tumor formation and progression through various mechanisms[23], including the activation of the cell cycle inhibitors p21 and p16INK4a, preventing the formation of Cyclin-dependent kinases-cyclin complexes during cell cycle progression, inducing stable G1 phase arrest, and is associated with increased senescence-associated β-galactosidase activity, changes in cell morphology, and metabolism[24,25]. Additionally, cellular senescence influences the tumor microenvironment by inducing a specific secretory phenotype, activating immune clearance mechanisms against tumors, and inducing drug resistance[26,27].

SCEL is a protein-coding gene that encodes a precursor for cornified envelope formation in terminally differentiated keratinized cells[28]. Using bioinformatics, Cheng et al. identified SCEL as a potential diagnostic and therapeutic target for PC, attributing its mechanism of action to the clonality and invasiveness of PC cells[21]. This protein is at the cell periphery and plays a role in the assembly and regulation of proteins in the cornified envelope[16]. Its LIM domains promote protein-protein interactions[29], regulate cell development processes, and serve as crucial nodes connecting protein function, signal transduction, and cell fate determination[30,31]. Moreover, as a unique zinc-finger protein domain, LIM is essential for maintaining cytoskeletal stability and regulating intercellular adhesion, which is vital for maintaining normal cellular functions and structural integrity[32]. With age, cytoskeletal stability is compromised, leading to a decline in cell function and promoting the aging process[33].

We found that SCEL was overexpressed in PC tissues and cell lines, correlating with poor clinical prognosis in patients with PC. Furthermore, our in vitro and in vivo studies indicated that reducing SCEL expression promoted PC cell senescence and inhibited PC cell proliferation, invasion, and metastasis. Immunoblotting and immunofluorescence analyses revealed negative correlations between SCEL and age-related proteins, suggesting that SCEL could serve as valuable diagnostic markers and therapeutic targets for PC. Moreover, the molecular mechanisms by which SCEL inhibits aging and promotes the proliferation, invasion, and metastasis of PC needs further investigation.

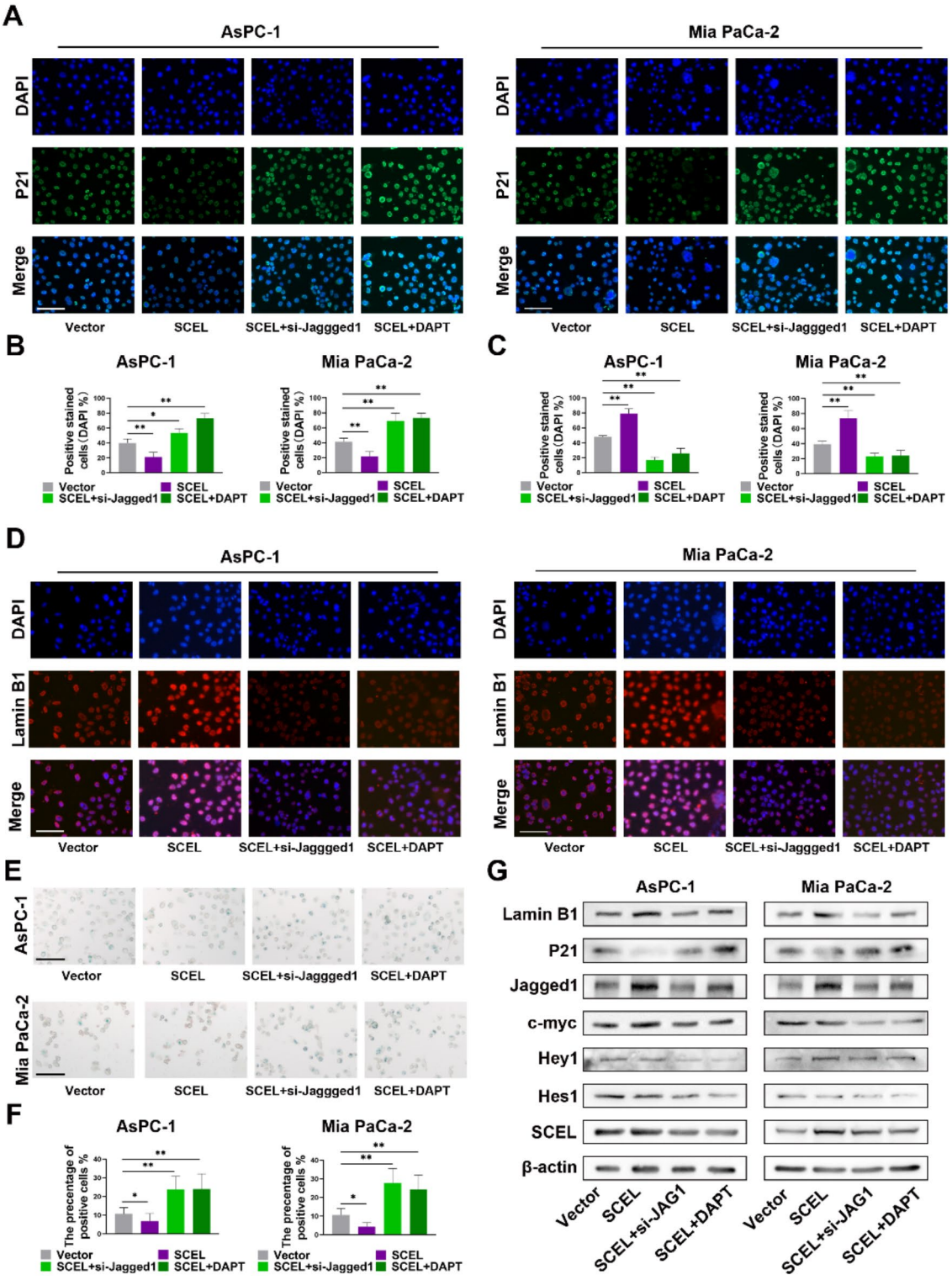

Fig. 6. Jagged-1's critical role in sciellin-induced senescence in pancreatic cells *in vitro*. The effects of Jagged-1 inhibition and Notch pathway inhibition on sciellin (SCEL)-driven cellular aging were evaluated in pancreatic cancer models (AsPC-1 and Mia PaCa-2 cells). Small interfering RNA targeting Jagged-1 (si-Jagged1) and Disitrubin Analog Peptide T, a Notch signaling inhibitor, were transfected into SCEL-overexpressing cells via a lentivirus. (**A–D**) Immunofluorescence assays assess senescence-associated protein levels and visually measure cellular aging. (**E**,**F**) *β*-Galactosidase staining highlighted senescent cells, further quantifying the senescence effect. (**G**) Western blot indicating detailed protein expression, suggesting molecular insights into pathway interactions. The data on the three biologically independent samples were analyzed using analysis of variance. *, **, ***, and **** represent $P < 0.05$, $P < 0.01$, $P < 0.001$, and $P < 0.0001$ significance levels.

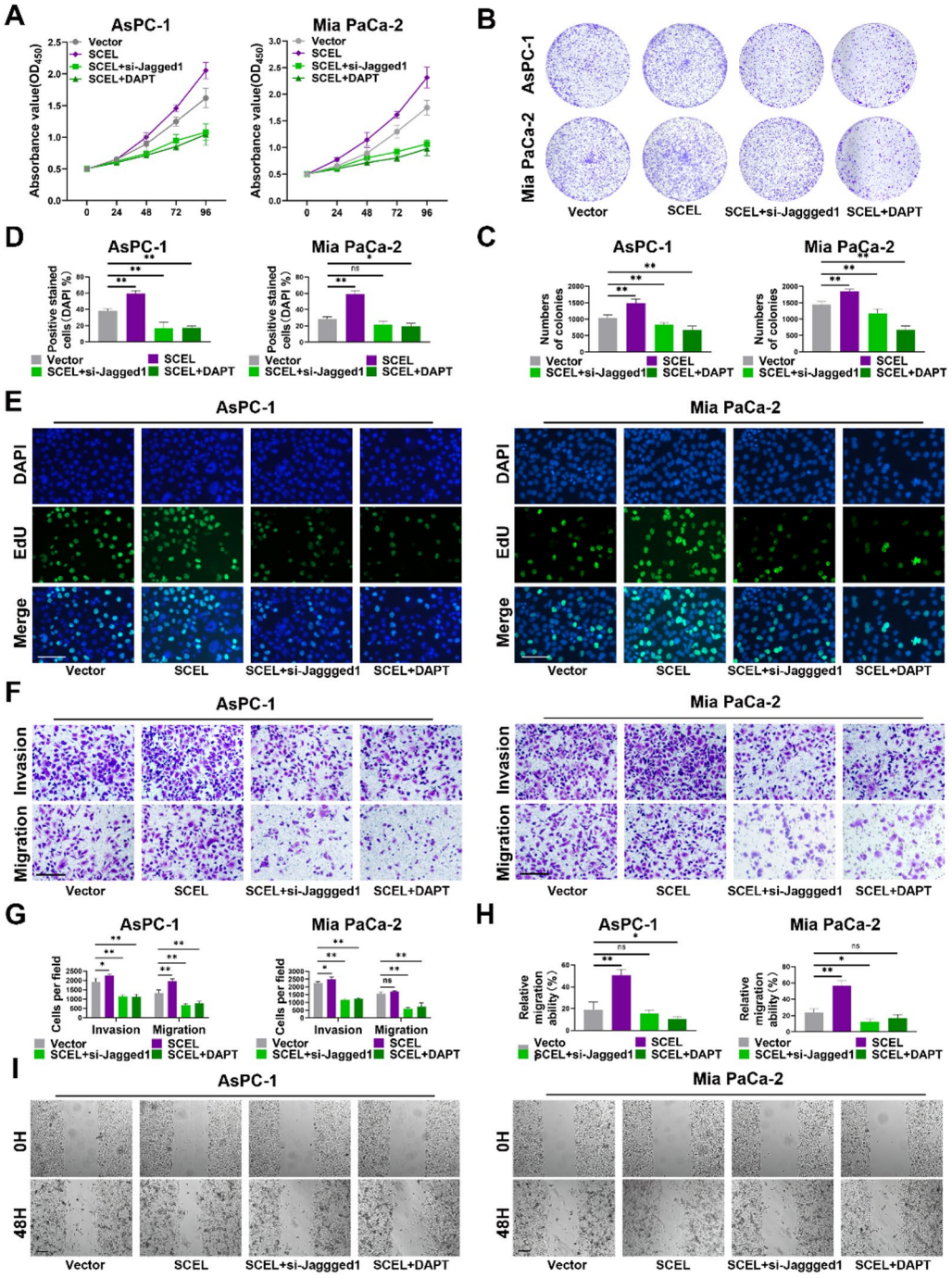

Fig. 7. Jagged-1's role in sciellin-driven proliferation and metastasis of pancreatic cancer cells in vivo. This figure shows the essential role of Jagged-1 in enhancing pancreatic cancer cell proliferation and metastasis facilitated by sciellin (SCEL) overexpression. Small interfering RNA targeting Jagged-1 (si-Jagged1) along with Disitrubin Analog Peptide T, a Notch pathway inhibitor, was used in AsPC-1 and Mia PaCa-2 cells overexpressing SCEL. (**A**) Cell proliferation was assessed using the cell counting kit-8 assay, which provides quantitative insights into cell growth. (**B**,**C**) Colony formation assay delineated the proliferative capacity of each cell group. (**D**,**E**) 5-Ethynyl-2′-deoxyuridine incorporation assay visually confirmed DNA synthesis, indicating active cell division. (**F**,**G**) Transwell assays demonstrate the invasive and migratory capabilities of these cells, which are crucial for their metastatic potential. (**H**,**I**) Wound healing assays were used to further quantify the migratory behavior of the cell groups. The data on the three biologically independent samples were analyzed using analysis of variance. *, **, ***, and **** represent $P<0.05$, $P<0.01$, $P<0.001$, and $P<0.0001$ significance levels.

Through Gene Set Enrichment Analysis (GSEA), we found that SCEL was closely associated with the Notch signaling pathway in PC cells, further validating that SCEL can activate downstream targets of the Notch pathway, including Hey1, Hes1, and c-myc. Previous studies have revealed that the Notch-sirtuin1-P21/P16 axis can induce cellular senescence, reducing the regenerative capacity of the liver[34], whereas Notch-1 or Jagged-1 overexpression can increase the replicative lifespan of endothelial cells, indicating a protective anti-aging effect[35]. Chen et al. reported that the Jagged-1/Notch-1 signaling pathway is a significant regulator of regeneration in various cell types, including cardiomyocytes, and that modulation of this pathway can have a significant anti-aging effect[15]. Moreover, during cellular senescence and tissue regeneration, the Notch pathway interacts with LIM proteins to jointly regulate the self-renewal and differentiation capacities of stem cells, which are crucial for maintaining tissue youthfulness and functional recovery[36,37].

We revealed that Jagged-1 is a key site in the Notch pathway, which is closely associated with SCEL. Validation analyses suggested that SCEL activated the Notch pathway by directly interacting with Jagged-1, with both exhibiting a positive correlation with its expression in PC cells and clinical tissues. Parry et al. reported that by specifically upregulating Jagged-1, the Notch pathway can autonomously and non-autonomously regulate the chromatin structure of aging cells through "trans-induction" of a unique aging phenotype in adjacent cells[38]. Studies have indicated that the activation of the Notch-1/Jagged-1 pathway can remove aging cells from the epidermis[39], and silencing of Jagged-1 or downstream genes of the Notch signaling pathway accelerates the senescence of microvascular endothelial cells[40]. Activation of Jagged1/Notch signaling inhibits stem cell aging, thereby increasing the osteogenic potential of mesenchymal stem cell sheets[41]. Therefore, Jagged-1 regulates cellular senescence and tissue regeneration, particularly aging-related tissue damage and regeneration, emphasizing the complexity of the Notch signaling pathway in regulating cellular senescence, suggesting that it is a potential therapeutic target for age-related diseases and cancers caused by cellular senescence.

Previous studies have revealed that Jagged-1 expression is often upregulated in PC[42] and promotes tumor growth and metastasis by activating a Notch-dependent feedback loop between PC cells and macrophages[43]. Our rescue experiments confirmed that SCEL inhibited PC senescence and promoted proliferation, invasion, and metastasis through Jagged-1, thus providing a novel perspective on the mechanism of action of SCEL in PC. In summary, our experimental results indicate that SCEL promotes its expression by interacting with Jagged-1 and activating the Notch signaling pathway, thereby inhibiting PC cell senescence and promoting PC cell proliferation, invasion, and metastasis. Our findings highlight the potential of SCELs a diagnostic marker and therapeutic targets in PC.

Data availability

The datasets during the current study are available from the corresponding author on reasonable request.

Received: 21 June 2024; Accepted: 28 January 2025
Published online: 08 May 2025

References

1. Kolbeinsson, H. M., Chandana, S., Wright, G. P. & Chung, M. Pancreatic Cancer: a review of current treatment and Novel therapies. *J. Invest. Surg.* **36**, 2129884 (2023).
2. Gaddam, S. et al. Incidence of pancreatic Cancer by Age and Sex in the US, 2000–2018. *Jama* **326**, 2075–2077 (2021).
3. Del Chiaro, M., Sugawara, T. & Karam, S. D. Messersmith, advances in the management of pancreatic cancer. *Bmj* **383**, e073995 (2023).
4. Hanahan, D. Hallmarks of Cancer: New dimensions. *Cancer Discov.* **12**, 31–46 (2022).
5. Moqri, M. et al. Validation of biomarkers of aging. *Nat. Med.* **30**, 360–372 (2024).
6. Zabransky, D. J. et al. Fibroblasts in the aged pancreas drive pancreatic cancer progression. *Cancer Res.* **84**, 1221–1236 (2024).
7. Billimoria, R. & Bhatt, P. Senescence in cancer: advances in detection and treatment modalities. *Biochem. Pharmacol.* **215**, 115739 (2023).
8. Schmitt, C. A., Wang, B. & Demaria, M. Senescence and cancer - role and therapeutic opportunities. *Nat. Rev. Clin. Oncol.* **19**, 619–636 (2022).
9. Cortesi, M. et al. Pancreatic cancer and cellular senescence: tumor microenvironment under the spotlight. *Int. J. Mol. Sci.* **23** (2021).
10. Gallahan, D. & Callahan, R. The mouse mammary tumor associated gene INT3 is a unique member of the NOTCH gene family (NOTCH4). *Oncogene* **14**, 1883–1890 (1997).
11. Shi, Q. et al. Notch signaling pathway in cancer: from mechanistic insights to targeted therapies. *Signal. Transduct. Target. Ther.* **9**, 128 (2024).
12. Bray, S. J. Notch signalling in context. *Nat. Rev. Mol. Cell. Biol.* **17**, 722–735 (2016).
13. Yan, W. et al. Notch Signaling regulates immunosuppressive Tumor-Associated macrophage function in pancreatic Cancer. *Cancer Immunol. Res.* **12**, 91–106 (2024).
14. Wu, X. et al. Ageing-exaggerated proliferation of vascular smooth muscle cells is related to attenuation of Jagged1 expression in endothelial cells. *Cardiovasc. Res.* **77**, 800–808 (2008).
15. Yoshida, Y. et al. Notch signaling regulates the lifespan of vascular endothelial cells via a p16-dependent pathway. *PLoS One.* **9**, e100359 (2014).
16. Champliaud, M. F., Burgeson, R. E., Jin, W., Baden, H. P. & Olson, P. F. cDNA cloning and characterization of sciellin, a LIM domain protein of the keratinocyte cornified envelope. *J. Biol. Chem.* **273**, 31547–31554 (1998).
17. Li, Y. et al. Role of Sciellin in gallbladder cancer proliferation and formation of neutrophil extracellular traps. *Cell. Death Dis.* **12**, 30 (2021).
18. Guo, H. et al. Sciellin promotes the development and progression of thyroid cancer through the JAK2/STAT3 signaling pathway. *Mol. Carcinog.* **63**, 701–713 (2024).
19. Chan, S. H., Kuo, W. H. & Wang, L. H. SCEL regulates switches between pro-survival and apoptosis of the TNF-α/TNFR1/NF-κB/c-FLIP axis to control lung colonization of triple negative breast cancer. *J. Biomed. Sci.* **30**, 93 (2023).
20. Jiang, B. et al. Down-regulation of long non-coding RNA HOTAIR promotes angiogenesis via regulating miR-126/SCEL pathways in burn wound healing. *Cell. Death Dis.* **11**, 61 (2020).

21. Cheng, Y. et al. Identification of candidate diagnostic and prognostic biomarkers for pancreatic carcinoma. *EBioMedicine* **40**, 382–393 (2019).
22. Gyawali, B. & Booth, C. M. Treatment of metastatic pancreatic cancer: 25 years of innovation with little progress for patients. *Lancet Oncol.* **25**, 167–170 (2024).
23. Moqri, M. et al. Biomarkers of aging for the identification and evaluation of longevity interventions. *Cell* **186**, 3758–3775 (2023).
24. Fakhri, S., Zachariah Moradi, S., DeLiberto, L. K. & Bishayee, A. Cellular senescence signaling in cancer: a novel therapeutic target to combat human malignancies. *Biochem. Pharmacol.* **199**, 114989 (2022).
25. Huang, W., Hickson, L. J., Eirin, A., Kirkland, J. L. & Lerman, L. O. Cellular senescence: the good, the bad and the unknown. *Nat. Rev. Nephrol.* **18**, 611–627 (2022).
26. Chambers, C. R., Ritchie, S., Pereira, B. A. & Timpson, P. Overcoming the senescence-associated secretory phenotype (SASP): a complex mechanism of resistance in the treatment of cancer. *Mol. Oncol.* **15**, 3242–3255 (2021).
27. Takasugi, M., Yoshida, Y., Hara, E. & Ohtani, N. The role of cellular senescence and SASP in tumour microenvironment. *Febs j.* **290**, 1348–1361 (2023).
28. Champliaud, M. F. et al. Gene characterization of sciellin (SCEL) and protein localization in vertebrate epithelia displaying barrier properties. *Genomics* **70**, 264–268 (2000).
29. Knöll, R. et al. The cardiac mechanical stretch sensor machinery involves a Z disc complex that is defective in a subset of human dilated cardiomyopathy. *Cell* **111**, 943–955 (2002).
30. Villalonga, E. et al. LIM Kinases, LIMK1 and LIMK2, Are Crucial Node Actors of the Cell Fate: Molecular to Pathological Features. *Cells* **12** (2023).
31. Klein, M. E. et al. PDLIM7 and CDH18 regulate the turnover of MDM2 during CDK4/6 inhibitor therapy-induced senescence. *Oncogene* **37**, 5066–5078 (2018).
32. Brown, M. C. & Turner, C. E. Paxillin: adapting to change. *Physiol. Rev.* **84**, 1315–1339 (2004).
33. Smith, M. A., Hoffman, L. M. & Beckerle, M. C. LIM proteins in actin cytoskeleton mechanoresponse. *Trends Cell. Biol.* **24**, 575–583 (2014).
34. Duan, J. L. et al. Shear stress-induced cellular senescence blunts liver regeneration through notch-sirtuin 1-P21/P16 axis. *Hepatology* **75**, 584–599 (2022).
35. Chen, L., Xia, W. & Hou, M. Mesenchymal stem cells attenuate doxorubicin–induced cellular senescence through the VEGF/Notch/TGF–β signaling pathway in H9c2 cardiomyocytes. *Int. J. Mol. Med.* **42**, 674–684 (2018).
36. Yuan, C., Wu, C., Xue, R., Jin, C. & Zheng, C. Suppression of human colon tumor by EERAC through regulating Notch/DLL4/Hes pathway inhibiting angiogenesis in vivo. *J. Cancer*. **12**, 5914–5922 (2021).
37. Gueta, K. et al. The stage-dependent roles of Ldb1 and functional redundancy with Ldb2 in mammalian retinogenesis. *Development* **143**, 4182–4192 (2016).
38. Parry, A. J. et al. NOTCH-mediated non-cell autonomous regulation of chromatin structure during senescence. *Nat. Commun.* **9**, 1840 (2018).
39. Yoshioka, H. et al. Senescent cell removal via JAG1-NOTCH1 signalling in the epidermis. *Exp. Dermatol.* **30**, 1268–1278 (2021).
40. Jo, H. R., Hwang, J. & Jeong, J. H. MicroRNA Mir-214-5p induces senescence of microvascular endothelial cells by targeting the JAG1/Notch signaling pathway. *Noncoding RNA Res.* **8**, 385–391 (2023).
41. Tian, Y. et al. Notch activation enhances mesenchymal stem cell sheet osteogenic potential by inhibition of cellular senescence. *Cell. Death Dis.* **8**, e2595 (2017).
42. Lee, J., Lee, J. & Kim, J. H. Association of Jagged1 expression with malignancy and prognosis in human pancreatic cancer. *Cell. Oncol. (Dordr)*. **43**, 821–834 (2020).
43. Geng, Y. et al. Notch-dependent inflammatory Feedback Circuit between macrophages and Cancer cells regulates pancreatic Cancer Metastasis. *Cancer Res.* **81**, 64–76 (2021).

Acknowledgements

We thank the Department of Hepatobiliary Surgery, The Affiliated Hospital of Guizhou Medical University, for technical support.

Author contributions

CH W, D L, and BB S designed and performed most of the experiments; ZW H and SY C analyzed the data and helped with the construction of the mouse model; CY S and C Y conceptualized the research and directed the study. All the authors have read and approved the final version of the manuscript.

Funding

This work was supported by the National Natural Science Foundation of China [No. 82373795 awarded to CS; No. 82360519 awarded to CY; No. 81960433 awarded to ZH]; The Project of Science and Technology of Guizhou Province [No. Qian Ke He Basic [2024] Youth 253]; and the Affiliated Hospital of Guizhou Medical University-National Natural Science Foundation of China Cultivation Program [No. gyfynsfc [2024]-40];2023 Discipline Leading Talent Project of affiliated Hospital of Guizhou Medical University [gyfyxkyc-2023-03]; Guizhou Province High-level Innovative Talents Training Plan "Hundred" level talents [grant number Qian Ke He Ping Tai Ren Cai GCC[2023] 082]; the Project of Science and Technology of Guizhou Province [No. Qian Ke He Zhi Cheng [2021] normal 080], and the Science and Technology Fund of the Guizhou Provincial Health and Family Planning Commission [No. gzwkj2023-031].

Declarations

Competing interests

The authors declare no competing interests.

Ethics statement

This study was approved by the Ethical Review at the Department of Hepatobiliary Surgery, The Affiliated Hospital of Guizhou Medical University (Guiyang, China).

Additional information

Supplementary Information The online version contains supplementary material available at https://doi.org/10.1038/s41598-025-88265-0.

Correspondence and requests for materials should be addressed to Z.H. or C.Y.

Reprints and permissions information is available at www.nature.com/reprints.

Publisher's note Springer Nature remains neutral with regard to jurisdictional claims in published maps and institutional affiliations.